GEOLOGY | THE GEOLOGICAL SOCIETY OF AMERICA®

https://doi.org/10.1130/G46998.1

Manuscript received 6 February 2019
Revised manuscript received 11 November 2019
Manuscript accepted 5 December 2019

Multi-stage arc magma evolution recorded by apatite in volcanic rocks

Chetan L. Nathwani[1,2], Matthew A. Loader[2], Jamie J. Wilkinson[2,1], Yannick Buret[2], Robert H. Sievwright[2] and Pete Hollings[3]

[1]Department of Earth Science and Engineering, Imperial College London, Exhibition Road, South Kensington Campus, London SW7 2AZ, UK

[2]London Centre for Ore Deposits and Exploration (LODE), Department of Earth Sciences, Natural History Museum, Cromwell Road, South Kensington, London SW7 5BD, UK

[3]Department of Geology, Lakehead University, 955 Oliver Road, Thunder Bay, Ontario P7B 5E1, Canada

ABSTRACT

Protracted magma storage in the deep crust is a key stage in the formation of evolved, hydrous arc magmas that can result in explosive volcanism and the formation of economically valuable magmatic-hydrothermal ore deposits. High magmatic water content in the deep crust results in extensive amphibole ± garnet fractionation and the suppression of plagioclase crystallization as recorded by elevated Sr/Y ratios and high Eu (high Eu/Eu*) in the melt. Here, we use a novel approach to track the petrogenesis of arc magmas using apatite trace element chemistry in volcanic formations from the Cenozoic arc of central Chile. These rocks formed in a magmatic cycle that culminated in high-Sr/Y magmatism and porphyry ore deposit formation in the Miocene. We use Sr/Y, Eu/Eu*, and Mg in apatite to track discrete stages of arc magma evolution. We apply fractional crystallization modeling to show that early-crystallizing apatite can inherit a high-Sr/Y and high-Eu/Eu* melt chemistry signature that is predetermined by amphibole-dominated fractional crystallization in the lower crust. Our modeling shows that crystallization of the in situ host-rock mineral assemblage in the shallow crust causes competition for trace elements in the melt that leads to apatite compositions diverging from bulk-magma chemistry. Understanding this decoupling behavior is important for the use of apatite as an indicator of metallogenic fertility in arcs and for interpretation of provenance in detrital studies.

INTRODUCTION

The chemical diversity observed in the rock record of volcanic arcs is determined by a multitude of processes operating between the magma source region and the surface. A fundamental step in producing this variability is fractional crystallization, assimilation, and melting in the lower crust which drive magmas to more evolved and hydrous compositions (Hildreth and Moorbath, 1988; Annen et al., 2006; Davidson et al., 2007). During extensive fractionation of hydrous magmas in the lower crust, amphibole (±garnet) is stabilized in the fractionating assemblage and plagioclase is suppressed (Müntener et al., 2001), resulting in melts with elevated Sr, an absence of strong negative Eu anomalies (both elements being compatible in plagioclase), and depleted Y (compatible in amphibole and garnet). Such magma evolution is promoted in strongly compressional, thickened arc crust and is commonly associated with porphyry Cu ore deposits because impeded magma ascent from the lower crust facilitates volatile accumulation and enrichment in ore-forming components (Chiaradia, 2015; Chiaradia and Caricchi, 2017). The high Sr/Y values that result can be used to provide insights into arc magma evolution (Macpherson et al., 2006; Rodriguez et al., 2007), evaluate whether a magmatic system has the potential to form a porphyry-related ore deposit in exploration (i.e., is "metallogenically fertile"; Richards, 2011; Loucks, 2014) and track crustal thickness (Chapman et al., 2015). However, this deep fractionation history may be obscured due to differentiation and mixing upon ascent to the shallow crust (Reubi and Blundy, 2009). Because arc rocks are a product of this multi-stage, polybaric process, unravelling the complete history of magmatic evolution using bulk-rock chemistry alone can be challenging. However, accessory minerals such as apatite are capable of capturing discrete periods of melt evolution during differentiation. For example, apatite has been shown to record the Sr content of the melt at the time of its crystallization, which has been used to reconstruct host-rock compositions in provenance studies (Jennings et al., 2011; Bruand et al., 2016).

In this study, we present a novel approach for understanding arc magma evolution by combining the trace element compositions of apatites from volcanic rocks with fractional crystallization modeling. We show that apatite records both deep crustal fractionation and shallow crustal crystallization processes, and tracks parameters valuable to understanding the generation of hydrous arc magmas and metallogenically fertile arcs.

STUDY AREA

The Andes of central Chile are an ideal region for a study of regional arc magma evolution and metallogeny because volcanic rock sequences (Fig. 1) record an extended period of subduction-related magmatism that culminated in high-Sr/Y magmatism (Sr/Y > 50) and the genesis of three major porphyry Cu deposits between 12.3 and 4.3 Ma (Perelló et al., 2012; Toro et al., 2012; Spencer et al., 2015): Los Pelambres, Rio Blanco–Los Bronces, and El Teniente (Kay and Mpodozis, 2001). This transition in magma chemistry has been attributed to shallowing of the subducting slab, linked to subduction of the Juan Fernández Ridge from ca. 26 Ma which led to substantial compression and crustal thickening that peaked at ca. 5 Ma (Stern and Skewes, 1995; Kay et al., 1999).

The studied volcanic formations are all calc-alkaline, were deposited between 124 and 3.9 Ma (Fig. 1B; Hollings et al., 2005), and

CITATION: Nathwani, C.L., et al., 2020, Multi-stage arc magma evolution recorded by apatite in volcanic rocks: Geology, v. 48, p. , https://doi.org/10.1130/G46998.1

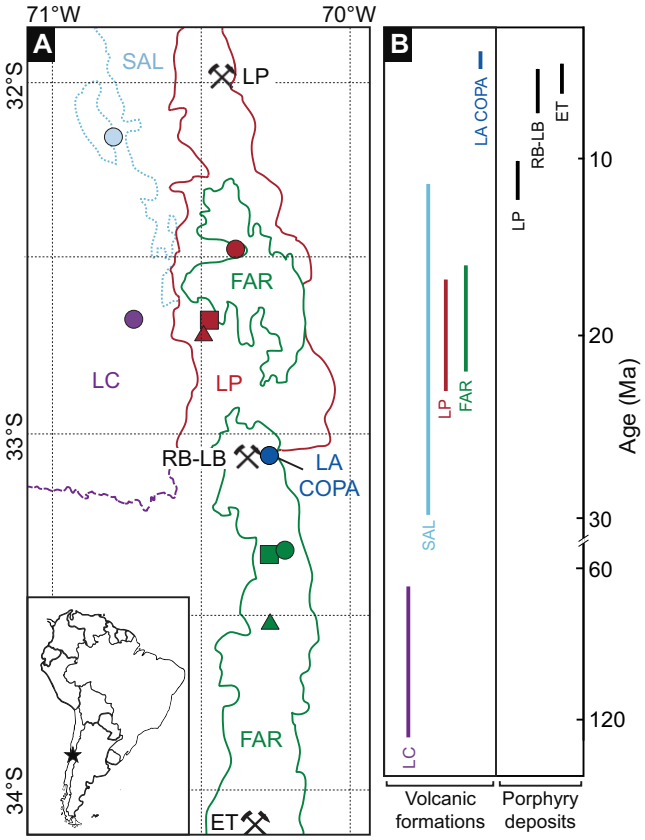

Figure 1. (A) Simplified map of studied volcanic units (FAR—Farellones Formation; LA COPA—La Copa Rhyolite; LC—Las Chilcas Formation; LP—Los Pelambres Formation; SAL—Salamanca Formation) in central Chile, with sample localities marked, and locations of major porphyry Cu-Mo deposits (LP—Los Pelambres; RB-LB—Rio Blanco–Los Bronces; ET—El Teniente). After Hollings et al. (2005). Inset: Location of study area in South America. (B) Published age ranges for formations studied (Rivano et al., 1993; Hollings et al., 2005; Piquer et al., 2017) and major porphyry Cu-Mo deposits (Perelló et al., 2012; Toro et al., 2012; Spencer et al., 2015).

represent magmas that followed different evolution paths in the arc crust. The Las Chilcas, Salamanca, Farellones, and Los Pelambres Formations show predominantly low Sr/Y (<50; Fig. 2) and pre-date the period of high-Sr/Y magmatism and mineralization (Fig. 1B). The Los Pelambres Formation displays some higher Sr/Y values that have been attributed to compression from localized shallowing of the subducting slab in this region (Yáñez et al., 2001). The La Copa Rhyolite is found in an immediately post-ore diatreme (ca. 4.5 Ma; Toro et al., 2012) at Rio Blanco–Los Bronces (Fig. 1A) and exhibits high Sr/Y, typical of the magmatism that generated mineralization.

SAMPLES AND METHODS

We present major and trace element analyses of apatites from a representative set of nine volcanic rock samples covering the period between the Cretaceous and Pliocene, both pre- and post-dating porphyry mineralization. Samples were collected distal from mineralization centers to minimize the effects of alteration on whole-rock and mineral chemistry. All samples have porphyritic texture, with compositions ranging from basaltic andesite to rhyolite (57–71 wt% SiO_2; Hollings et al., 2005). The studied samples are all derived from lavas with the exception of the La Copa Rhyolite diatreme. The occurrence of apatite as inclusions in clinopyroxene and amphibole, and apatite saturation temperatures (Harrison and Watson, 1984) that typically exceed 900°C, suggest that apatite is a relatively early-saturating phase in the samples. Major elements in apatite were determined by electron microprobe and trace elements by laser ablation inductively coupled plasma mass spectrometry at the Natural History Museum, London (UK). Detailed rock descriptions, data tables, and additional information on the analytical methods are provided in the GSA Data Repository[1].

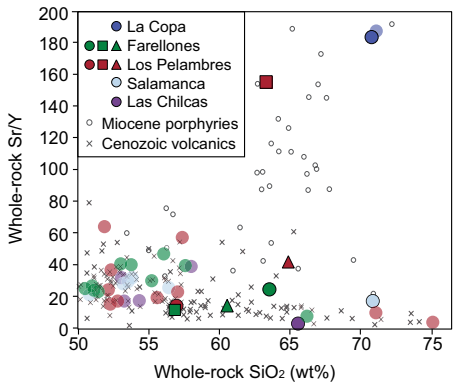

Figure 2. Whole-rock SiO_2 and Sr/Y for the studied central Chilean volcanic units (Hollings et al., 2005) with additional data from other Cenozoic central Chilean volcanics (Piquer et al., 2017) and Miocene porphyry Cu-Mo intrusives from Los Pelambres, Rio Blanco–Los Bronces, and El Teniente (Stern and Skewes, 1995; Reich et al., 2003; Stern et al., 2011). Opaque symbols with black outlines are samples used in this study. Farellones Formation: samples CA-28 (circle), CA-29 (square), CV-12 (triangle). Los Pelambres Formation: samples CN-11 (circle), CN-37 (square), CN-40 (triangle). Faded colored symbols represent samples from Hollings et al. (2005) that were not used in this study.

APATITE TRACE ELEMENT COMPOSITIONS

Apatite Sr and Y show a broad negative correlation (Fig. 3) and exhibit both differences between samples (inter-sample) and within-sample trends (intra-sample). Apatite Sr/Y (Sr/Y_{ap}) varies between 0.1 and 11 (Fig. 4A), with low Sr/Y_{ap} (<2) present in the most mafic (<61% SiO_2) and felsic (>70%) samples, and higher Sr/Y_{ap} (>2) exclusively found in the intermediary whole-rock compositions (62%–66% SiO_2). The highest Sr/Y_{ap} cannot be explained by high Sr alone, but requires reduced Y concentrations (<200 ppm; Fig. 3), and thus any mechanism to explain the presence of high Sr/Y_{ap} must account for the simultaneous enrichment in Sr and depletion in Y. A correlation between Sr/Y_{ap} and Eu/Eu^*_{ap} is present that forms a well-defined logarithmic curve, in which samples from the Farellones and Los Pelambres Formations display higher Eu/Eu^*_{ap} (Eu/Eu^*_{ap} >0.5) and the La Copa, Salamanca, and Las Chilcas samples exhibit lower values (Fig. 4A).

Experimental work shows that Mg in apatite (Mg_{ap}) is proportional to the Mg content of the melt (Prowatke and Klemme, 2006), which suggests that Mg_{ap} can be used as a tracer of magmatic differentiation during apatite crystallization. Using this approach, our data reveal three systematic intra-sample trends in Sr/Y_{ap} with magmatic differentiation (Fig. 4B). Within samples, decreasing Sr/Y_{ap} with differentiation (decreasing Mg_{ap}) occurs where Sr/Y_{ap} is initially elevated. Conversely, where Sr/Y_{ap} is initially low, it remains low with differentiation.

Trends in igneous apatite chemistry can reflect: (1) changes in primitive melt composition; (2) changes in the trace element budget of the melt during fractional crystallization; (3) varying thermodynamic and compositional influences on apatite-melt partitioning; and/or (4) re-equilibration during near-solidus magma storage or hydrothermal alteration. Apatites analyzed here are predominantly fluorapatite with light rare earth element enrichment and

[1]GSA Data Repository item 2020086, supplementary chemical diagrams, images, modeling methodology, and sample descriptions, Dataset DR1 (analyses of Durango apatite standard), and Dataset DR2 (whole-rock electron probe microanalysis and laser ablation–inductively coupled–mass spectrometry apatite data), is available online at http://www.geosociety.org/datarepository/2020/, or on request from editing@geosociety.org.

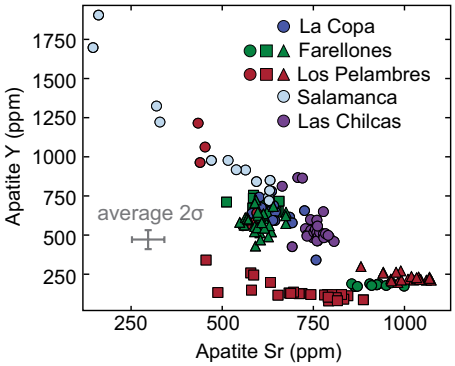

Figure 3. Sr versus Y compositions of apatites analyzed in this study (from central Chile) showing broad negative correlation, indicating that changes in Sr/Y in apatite are controlled by variation in both Sr and Y. Refer to the Figure 2 caption for sample numbers.

negative Eu anomalies (Data Repository), consistent with an igneous origin (Piccoli and Candela, 2002). Cathodoluminescence images show igneous zoning features and not the irregular patchy zoning, porous textures, and secondary rare earth element mineral growth that characterize hydrothermal origins or alteration (Bouzari et al., 2016). Hence, we preclude hydrothermal effects as a major control on the observed trends. Although melt composition and temperature influence apatite-melt partition coefficients, they do not significantly affect partition coefficient ratios. For example, $(D_{Sr}/D_Y)_{ap}$ (D—distribution coefficient) does not vary systematically with changing melt composition ($[D_{Sr}/D_Y]_{ap}$ = 0.5–1.0; Prowatke and Klemme, 2006) and therefore would have little systematic effect on Sr/Y_{ap}. Although we cannot exclude compositional variation in the primitive magmas involved, the restricted range in Sr/Y of the most primitive rocks in the region (Fig. 2) suggests that source variation is unlikely to have had a significant effect on Sr/Y_{ap}. Thus, we consider the trends in our data as having been primarily controlled by melt evolution during crustal transit.

APATITE AS A TRACER OF DEEP CRUSTAL EVOLUTION

Because intra-sample trends of increasing Sr/Y_{ap} with differentiation are not observed (Fig. 4B), we infer that elevated Sr/Y_{ap} signatures in apatite are produced by a magmatic process occurring prior to apatite crystallization. Higher whole-rock Sr/Y (>20; Fig. 2) of the samples with high Sr/Y_{ap} suggests a fractional crystallization process that affected both bulk-magma and mineral chemistry. High Sr/Y_{melt} is readily generated in the deep crust through fractionation of an amphibole (±garnet) assemblage in high-pressure, hydrous magmas (Richards and Kerrich, 2007), and the lower compatibility of Eu over Sm and Gd in amphibole at typical oxygen fugacity, f_{O_2}, (nickel-nickel oxide [NNO]; Nandedkar et al., 2016) produces a concomitant increase in Eu/Eu*$_{melt}$. Although apatite is unlikely to crystallize under such conditions and compositions (Nandedkar et al., 2014), it may inherit these elevated Sr/Y_{melt} and Eu/Eu*$_{melt}$ signatures upon near-liquidus crystallization in the shallow crust.

To investigate the sensitivity of apatite chemistry to deep crustal magmatic evolution, we developed a Rayleigh trace element fractionation model (Figs. 4A and 4B; see the Data Repository for further model details). We estimated an initial melt composition from the apatite compositions of the most primitive sample (CA-29) using apatite-melt partition coefficients (Prowatke and Klemme, 2006). We modeled progressive deep crustal fractionation from this primitive melt using phase proportions appropriate for the deep crust (66% amphibole, 33% clinopyroxene; Melekhova et al., 2014) and calculated the composition of residual melts. Lastly, we calculated new apatite compositions in equilibrium with the fractionated melts at each step (Figs. 4A and 4B). The maximum Sr/Y_{ap} and Eu/Eu*$_{ap}$ values in our data are produced by fractionation of ~60% of the deep crustal assemblage from the initial primitive melt, consistent with the typical degree of deep crustal fractionation calculated from experimental data and modeling (Richards and Kerrich, 2007; Nandedkar et al., 2014).

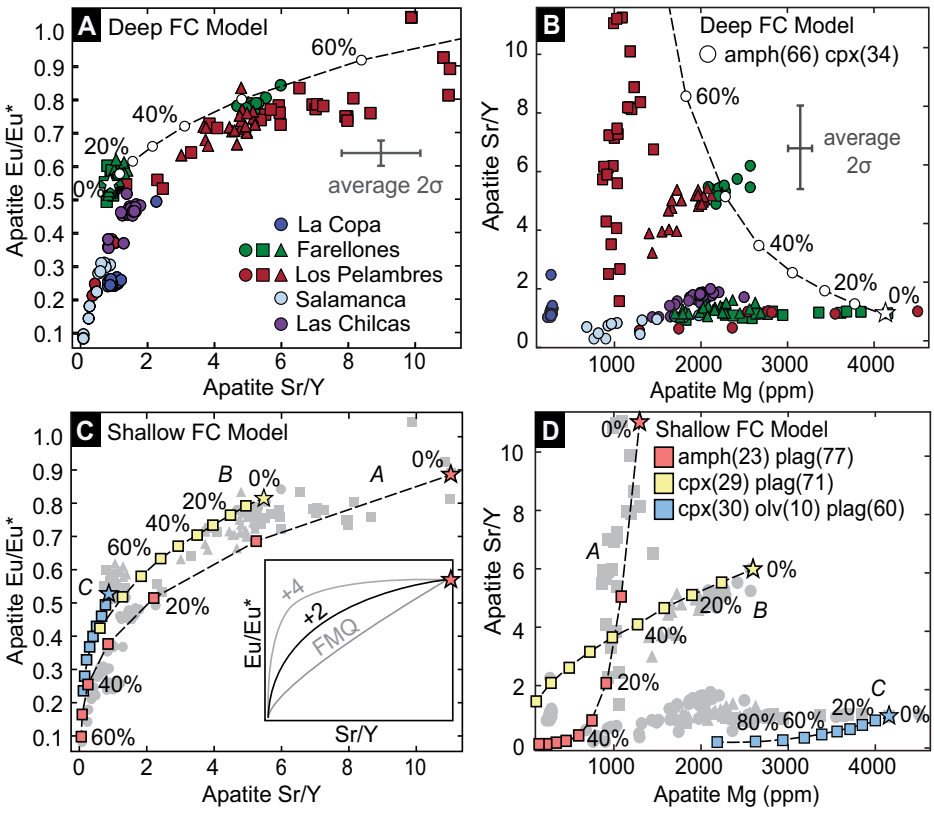

Figure 4. Apatite trace element compositions and trace element fractional crystallization (FC) models for samples analyzed in this study (from central Chile). (A) Apatite Sr/Y versus apatite Eu/Eu*. Open circles and dashed line show theoretical apatite compositions in equilibrium with modeled melts produced from fractional crystallization in deep crust. Labeled percentage values indicate the percentage of crystallization of the deep FC mineral assemblage (deep FC model, 66% amphibole [amph], 34% clinopyroxene [cpx]). (B) Apatite Sr/Y versus apatite Mg. Compositional differences are visible between samples (inter-sample), and there are distinct trends within individual samples (intra-sample). (C) Modeled apatite Eu/Eu* and Sr/Y in shallow crustal fractional crystallization model (shallow FC model). Models are run at FMQ (fayalite-magnetite-quartz); inset shows simplified version of figure with alternative models of path A (gray lines) at different f_{O_2} values (at FMQ and at FMQ + 4). (D) Modeled apatite Sr/Y and Mg in shallow crustal fractional crystallization model. For panels C and D, gray symbols show natural apatite data from this study; percentage values indicate percentage of crystallization of the mineral assemblage in each model. Mineral assemblage proportions are those estimated from the host samples of apatite at the start of each path (model A: 23% amphibole [amph], 77% plagioclase [plag]; model B: 29% clinopyroxene [cpx], 71% plagioclase; model C: 30% clinopyroxene, 10% olivine [olv], 60% plagioclase).

SHALLOW CRUSTAL DIFFERENTIATION CONTROLS ON APATITE CHEMISTRY

Although inter-sample differences in Sr/Y_{ap} and Eu/Eu*$_{ap}$ in the earliest-crystallizing apatites in each sample can be explained by variable deep crustal fractionation, the intra-sample variations of these values with Mg_{ap} are likely

to have resulted from apatite co-crystallization with the phenocryst assemblages forming in the shallow crust. The compatibility of Sr and Eu in plagioclase, and the abundance of plagioclase as a phenocryst phase, mean that plagioclase crystallization is a likely mechanism for lowering Sr/Y_{melt} and Eu/Eu^*_{melt} during shallow crustal melt evolution. We tested this hypothesis by modeling the in situ evolution of three melts (pathways A, B, and C; Figs. 4C and 4D) and the apatite compositions in equilibrium with them. These trajectories were calculated by: (1) estimating a starting melt composition from the earliest-crystallizing apatite (highest Mg_{ap}) on each trend; (2) crystallization of successively increasing proportions of the phenocryst phases observed in the host rocks of these apatites; and (3) recalculating the apatite compositions in equilibrium with the residual melts at each step. In each case, the crystallization of the phenocryst assemblage in the rock produced apatite compositions consistent with the observed intra-sample Sr/Y_{ap} and Eu/Eu^*_{ap} trends. The curvature of the modeled Sr/Y_{ap} and Eu/Eu^*_{ap} relationship is sensitive to magmatic oxidation state (Fig. 4C inset), and best reproduces the natural apatite data at two log units (±1) above the fayalite-magnetite-quartz (FMQ) redox buffer, a typical value for arc magmas (e.g., Carmichael, 1991).

Thus, we suggest that apatites crystallized closest to the liquidus capture the signature of deep crustal magma evolution that is coupled to whole-rock chemistry, and that this stage defines the inter-sample variations in our data set. Conversely, later-crystallizing apatites compete for trace elements with co-crystallizing mineral phases in the shallow crust and thereby track a chemical divergence of the melt from bulk-rock compositions (e.g., Miles et al., 2013), as recorded by the intra-sample trends.

IMPLICATIONS FOR APATITE AS A PETROGENETIC TOOL

The utility of apatite in provenance studies relies on its ability to reflect host-rock chemistry (Belousova et al., 2002; Jennings et al., 2011; Bruand et al., 2016). Here, we show that although higher Sr/Y_{ap} and Eu/Eu^*_{ap} in the Los Pelambres and Farellones samples are observed, reflecting the higher whole-rock Sr/Y and Eu/Eu* of the host samples (Fig. 2), this signature is preserved only in the earliest-crystallizing, near-liquidus apatites (high Mg_{ap}). The La Copa Rhyolite has the highest whole-rock Sr/Y, but consistently low Sr/Y_{ap} which we interpret to reflect late apatite crystallization (low Mg_{ap}) after significant shallow plagioclase crystallization in the shallow crust (Figs. 4C and 4D). Consequently, caution should be exercised when using apatite to reconstruct rock compositions (e.g., for provenance or metallogenic fertility studies), because the ability of apatite to reflect bulk-rock and/or deep crustal chemical signatures is dependent on its timing of crystallization relative to other mineral phases. Therefore Mg_{ap} is a key parameter in helping to properly interpret igneous apatite chemistry data in petrogenetic studies.

SUMMARY AND CONCLUSIONS

We demonstrate that apatite in volcanic rocks can track crustal-scale magmatic evolution by recording both deep crustal bulk-magma differentiation and shallow crustal melt evolution. Apatite tracks parameters (Mg, Sr/Y, and Eu/Eu*) that indicate the development of the evolved, hydrous and oxidized magma compositions thought to be required for metallogenic fertility in arcs. We suggest that our approach is widely applicable for unravelling the composite evolution of arc magmas and studying magmatic processes conducive to porphyry ore deposit formation.

ACKNOWLEDGMENTS

We thank J. Spratt, W. Brownscombe, and E. Brugge for analytical assistance. Our modeling benefited greatly from discussions with J. Blundy. This work was financially supported by the Department of Earth Science and Engineering, Imperial College London, and by the Imaging and Analysis Centre and LODE Laboratory, Natural History Museum, London. Wilkinson, Buret, and Sievwright acknowledge funding under Natural Environment Research Council grant NE/P017452/1, "From arc magmas to ores (FAMOS): A mineral systems approach". We thank D. Brown for editorial handling and A. Miles and two anonymous reviewers for their constructive reviews.

REFERENCES CITED

Annen, C., Blundy, J.D., and Sparks, R.S.J., 2006, The genesis of intermediate and silicic magmas in deep crustal hot zones: Journal of Petrology, v. 47, p. 505–539, https://doi.org/10.1093/petrology/egi084.

Belousova, E.A., Griffin, W.L., O'Reilly, S.Y., and Fisher, N.I., 2002, Apatite as an indicator mineral for mineral exploration: Trace-element compositions and their relationship to host rock type: Journal of Geochemical Exploration, v. 76, p. 45–69, https://doi.org/10.1016/S0375-6742(02)00204-2.

Bouzari, F., Hart, C.J.R., Bissig, T., and Barker, S., 2016, Hydrothermal alteration revealed by apatite luminescence and chemistry: A potential indicator mineral for exploring covered porphyry copper deposits: Economic Geology and the Bulletin of the Society of Economic Geologists, v. 111, p. 1397–1410, https://doi.org/10.2113/econgeo.111.6.1397.

Bruand, E., Storey, C., and Fowler, M., 2016, An apatite for progress: Inclusions in zircon and titanite constrain petrogenesis and provenance: Geology, v. 44, p. 91–94, https://doi.org/10.1130/G37301.1.

Carmichael, I.S.E., 1991, The redox states of basic and silicic magmas: A reflection of their source regions?: Contributions to Mineralogy and Petrology, v. 106, p. 129–141, https://doi.org/10.1007/BF00306429.

Chapman, J.B., Ducea, M.N., DeCelles, P.G., and Profeta, L., 2015, Tracking changes in crustal thickness during orogenic evolution with Sr/Y: An example from the North American Cordillera: Geology, v. 43, p. 919–922, https://doi.org/10.1130/G36996.1.

Chiaradia, M., 2015, Crustal thickness control on Sr/Y signatures of recent arc magmas: An Earth scale perspective: Scientific Reports, v. 5, 8115, https://doi.org/10.1038/srep08115.

Chiaradia, M., and Caricchi, L., 2017, Stochastic modelling of deep magmatic controls on porphyry copper deposit endowment: Scientific Reports, v. 7, 44523, https://doi.org/10.1038/srep44523.

Davidson, J., Turner, S., Handley, H., Macpherson, C., and Dosseto, A., 2007, Amphibole "sponge" in arc crust?: Geology, v. 35, p. 787–790, https://doi.org/10.1130/G23637A.1.

Harrison, T.M., and Watson, E.B., 1984, The behavior of apatite during crustal anatexis: Equilibrium and kinetic considerations: Geochimica et Cosmochimica Acta, v. 48, p. 1467–1477, https://doi.org/10.1016/0016-7037(84)90403-4.

Hildreth, W., and Moorbath, S., 1988, Crustal contributions to arc magmatism in the Andes of Central Chile: Contributions to Mineralogy and Petrology, v. 98, p. 455–489, https://doi.org/10.1007/BF00372365.

Hollings, P., Cooke, D., and Clark, A., 2005, Regional geochemistry of tertiary igneous rocks in central Chile: Implications for the geodynamic environment of giant porphyry copper and epithermal gold mineralization: Economic Geology and the Bulletin of the Society of Economic Geologists, v. 100, p. 887–904, https://doi.org/10.2113/gsecongeo.100.5.887.

Jennings, E.S., Marschall, H.R., Hawkesworth, C.J., and Storey, C.D., 2011, Characterization of magma from inclusions in zircon: Apatite and biotite work well, feldspar less so: Geology, v. 39, p. 863–866, https://doi.org/10.1130/G32037.1.

Kay, S.M., and Mpodozis, C., 2001, Central Andean ore deposits linked to evolving shallow subduction systems and thickening crust: GSA Today, v. 11, no. 3, p. 4–9, https://doi.org/10.1130/1052-5173(2001)011<0004:CAODLT>2.0.CO;2.

Kay, S.M., Mpodozis, C., and Coira, B., 1999, Neogene magmatism, tectonism, and mineral deposits of the central Andes (22° to 33° S latitude), *in* Skinner, B.J., ed., Geology and Ore Deposits of the Central Andes: Society of Economic Geologists Special Publication 7, p. 27–59, https://doi.org/10.5382/SP.07.02.

Loucks, R.R., 2014, Distinctive composition of copper-ore-forming arc magmas: Australian Journal of Earth Sciences, v. 61, p. 5–16, https://doi.org/10.1080/08120099.2013.865676.

Macpherson, C.G., Dreher, S.T., and Thirlwall, M.F., 2006, Adakites without slab melting: High pressure differentiation of island arc magma, Mindanao, the Philippines: Earth and Planetary Science Letters, v. 243, p. 581–593, https://doi.org/10.1016/j.epsl.2005.12.034.

Melekhova, E., Blundy, J., Robertson, R., and Humphreys, M.C.S., 2014, Experimental evidence for polybaric differentiation of primitive arc basalt beneath St. Vincent, Lesser Antilles: Journal of Petrology, v. 56, p. 161–192, https://doi.org/10.1093/petrology/egu074.

Miles, A.J., Graham, C.M., Hawkesworth, C.J., Gillespie, M.R., and Hinton, R.W., 2013, Evidence for distinct stages of magma history recorded by the compositions of accessory apatite and zircon: Contributions to Mineralogy and Petrology, v. 166, p. 1–19, https://doi.org/10.1007/s00410-013-0862-9.

Müntener, O., Kelemen, P.B., and Grove, T.L., 2001, The role of H_2O during crystallization of primitive arc magmas under uppermost mantle conditions and genesis of igneous pyroxenites: An experimental study: Contributions to Mineralogy and Petrology, v. 141, p. 643–658, https://doi.org/10.1007/s004100100266.

Nandedkar, R.H., Ulmer, P., and Müntener, O., 2014, Fractional crystallization of primitive, hydrous

arc magmas: An experimental study at 0.7 GPa: Contributions to Mineralogy and Petrology, v. 167, 1015, https://doi.org/10.1007/s00410-014-1015-5.

Nandedkar, R.H., Hürlimann, N., Ulmer, P., and Müntener, O., 2016, Amphibole–melt trace element partitioning of fractionating calc-alkaline magmas in the lower crust: An experimental study: Contributions to Mineralogy and Petrology, v. 171, 71, https://doi.org/10.1007/s00410-016-1278-0.

Perelló, J., Sillitoe, R.H., Mpodozis, C., Brockway, H., and Posso, H., 2012, Geologic setting and evolution of the porphyry copper-molybdenum and copper-gold deposits at Los Pelambres, central Chile, *in* Hedenquist, J.W., et al., eds., Geology and Genesis of Major Copper Deposits and Districts of the World: A Tribute to Richard H. Sillitoe: Society of Economic Geologists Special Publication, 16, p. 79–104.

Piccoli, P.M., and Candela, P.A., 2002, Apatite in igneous systems: Reviews in Mineralogy and Geochemistry, v. 48, p. 255–292, https://doi.org/10.2138/rmg.2002.48.6.

Piquer, J., Hollings, P., Rivera, O., Cooke, D.R., Baker, M., and Testa, F., 2017, Along-strike segmentation of the Abanico Basin, central Chile: New chronological, geochemical and structural constraints: Lithos, v. 268–271, p. 174–197, https://doi.org/10.1016/j.lithos.2016.10.025.

Prowatke, S., and Klemme, S., 2006, Trace element partitioning between apatite and silicate melts: Geochimica et Cosmochimica Acta, v. 70, p. 4513–4527, https://doi.org/10.1016/j.gca.2006.06.162.

Reich, M., Parada, M.A., Palacios, C., Dietrich, A., Schultz, F., and Lehmann, B., 2003, Adakite-like signature of Late Miocene intrusions at the Los Pelambres giant porphyry copper deposit in the Andes of central Chile: Metallogenic implications: Mineralium Deposita, v. 38, p. 876–885, https://doi.org/10.1007/s00126-003-0369-9.

Reubi, O., and Blundy, J., 2009, A dearth of intermediate melts at subduction zone volcanoes and the petrogenesis of arc andesites: Nature, v. 461, p. 1269–1273, https://doi.org/10.1038/nature08510.

Richards, J.P., 2011, High Sr/Y arc magmas and porphyry Cu ± Mo ± Au deposits: Just add water: Economic Geology and the Bulletin of the Society of Economic Geologists, v. 106, p. 1075–1081, https://doi.org/10.2113/econgeo.106.7.1075.

Richards, J.P., and Kerrich, R., 2007, Special paper: Adakite-like rocks: Their diverse origins and questionable role in metallogenesis: Economic Geology and the Bulletin of the Society of Economic Geologists, v. 102, p. 537–576, https://doi.org/10.2113/gsecongeo.102.4.537.

Rivano, S.O., Sepulveda, S., Boric, R., and Espineria, D., 1993, Carta geológica de Chile, hojas Quillota y Portillo, V Región: Santiago, Chile, Servicio Nacional de Geología y Minería, Carta Geológica de Chile 73, scale 1:250,000.

Rodríguez, C., Sellés, D., Dungan, M., Langmuir, C., and Leeman, W., 2007, Adakitic dacites formed by intracrustal crystal fractionation of water-rich parent magmas at Nevado de Longaví volcano (36.2°S; Andean Southern Volcanic Zone, central Chile): Journal of Petrology, v. 48, p. 2033–2061, https://doi.org/10.1093/petrology/egm049.

Spencer, E.T., Wilkinson, J.J., Creaser, R.A., and Seguel, J., 2015, The distribution and timing of molybdenite mineralization at the El Teniente Cu-Mo porphyry deposit, Chile: Economic Geology and the Bulletin of the Society of Economic Geologists, v. 110, p. 387–421, https://doi.org/10.2113/econgeo.110.2.387.

Stern, C.R., and Skewes, M.A., 1995, Miocene to present magmatic evolution at the northern end of the Andean Southern Volcanic Zone, Central Chile: Revista Geológica de Chile, v. 22, p. 261–272.

Stern, C.R., Skewes, M.A., and Arévalo, A., 2011, Magmatic evolution of the giant El Teniente Cu-Mo deposit, central Chile: Journal of Petrology, v. 52, p. 1591–1617, https://doi.org/10.1093/petrology/egq029.

Toro, J.C., Ortúzar, J., Zamorano, J., Cuadra, P., Hermosilla, J., and Spröhnle, C., 2012, Protracted magmatic-hydrothermal history of the Río Blanco–Los Bronces District, central Chile: Development of world's greatest known concentration of copper, *in* Hedenquist, J.W., et al., eds., Geology and Genesis of Major Copper Deposits and Districts of the World: A Tribute to Richard H. Sillitoe: Society of Economic Geologists Special Publication, v. 16, p. 105–126.

Yáñez, G.A., Ranero, C.R., von Huene, R., and Díaz, J., 2001, Magnetic anomaly interpretation across the southern central Andes (32°–34°S): The role of the Juan Fernández Ridge in the late Tertiary evolution of the margin: Journal of Geophysical Research, v. 106, p. 6325–6345, https://doi.org/10.1029/2000JB900337.

Printed in USA